

LA-UR- 95 - 872

*Title:* Plasma Source Ion Implantation of Metal Ions:  
Synchronization of Cathodic-Arc Plasma Production  
and Target Bias Pulses

*Author(s):* Blake P. Wood  
William A. Reass  
Ivars Henins

*Submitted to:* Second International Workshop on Plasma Based Ion  
Implantation



**Los Alamos**  
NATIONAL LABORATORY

Los Alamos National Laboratory, an affirmative action/equal opportunity employer, is operated by the University of California for the U.S. Department of Energy under contract W-7405-ENG-36. By acceptance of this article, the publisher recognizes that the U.S. Government retains a nonexclusive, royalty-free license to publish or reproduce the published form of this contribution, or to allow others to do so, for U.S. Government purposes. The Los Alamos National Laboratory requests that the publisher identify this article as work performed under the auspices of the U.S. Department of Energy.

**MASTER**

Form No. 836 R5  
ST 2629 10/91

## **DISCLAIMER**

**Portions of this document may be illegible in electronic image products. Images are produced from the best available original document.**

## DISCLAIMER

This report was prepared as an account of work sponsored by an agency of the United States Government. Neither the United States Government nor any agency thereof, nor any of their employees, makes any warranty, express or implied, or assumes any legal liability or responsibility for the accuracy, completeness, or usefulness of any information, apparatus, product, or process disclosed, or represents that its use would not infringe privately owned rights. Reference herein to any specific commercial product, process, or service by trade name, trademark, manufacturer, or otherwise does not necessarily constitute or imply its endorsement, recommendation, or favoring by the United States Government or any agency thereof. The views and opinions of authors expressed herein do not necessarily state or reflect those of the United States Government or any agency thereof.

---

# Plasma Source Ion Implantation of Metal Ions: Synchronization of Cathodic-Arc Plasma Production and Target Bias Pulses

B. P. Wood, W. A. Reass, and I. Henins

Los Alamos National Laboratory, Los Alamos, NM 87545

## Abstract

An erbium cathodic-arc has been installed on a Plasma Source Ion Implantation (PSII) experiment to allow the implantation of erbium metal and the growth of adherent erbia (erbium oxide) films on a variety of substrates. Operation of the PSII pulser and the cathodic-arc are synchronized to achieve pure implantation, rather than the hybrid implantation/deposition being investigated in other laboratories. The relative phase of the 20  $\mu$ s PSII and cathodic-arc pulses can be adjusted to tailor the energy distribution of implanted ions and suppress the initial high-current drain on the pulse modulator. We present experimental data on this effect and make a comparison to results from particle-in-cell simulations

## 1 Introduction

In Plasma Source Ion Implantation (PSII), an object is placed in a plasma containing the ions of interest, and then pulsed to a high negative voltage, accelerating the positive ions toward the object and implanting them in its surface [1]. This is commonly performed with gaseous plasmas [2, 3, 4]. Recently, this process has been applied with metal-ion plasmas formed by cathodic-arc ([5, 6] for metal PSII, [7, 8] for cathodic-arcs), typically as a hybrid implantation/deposition process with long (millisecond) cathodic-arc pulses and short (microsecond) target bias pulses. In this paper we describe research being conducted at Los Alamos National Laboratory, in which we have added a cathodic-arc running erbium to our large-scale PSII facility [10, 9], synchronizing the cathodic-arc and target bias pulses so as to achieve a pure metal-ion implantation at high voltage. Our goal in this work is to increase the adherence of ceramic metal-oxide layers deposited conformally on substrates of complicated shape.

## 2 Experimental Equipment

Our cathodic-arc, shown schematically in Figure 1, is constructed from an electrical feedthrough which fits on a 2 3/4" conflat flange. A 21 mm inner-diameter anode has been welded to the vacuum side of the conflat. A 5.5 mm diameter cathode fits inside a thin alumina sleeve. A trigger wire is wrapped around the end of the alumina sleeve, and passes through a hole drilled in the conflat. This hole is vacuum sealed with epoxy. No cathode cooling, magnetic nozzling of the plasma or filtering of macroparticles is currently performed.

The cathodic-arc is driven by a solid-state pulse modulator designed by one of the authors (Reass). It is based on a Powerex CM400HA-24H insulated gate bipolar transistor (IGBT) rated at 1200 V and 800 A, and is driven with a 1 kW dc power supply. A 10 mJ trigger pulse is stepped up to 10 kV with a small transformer. This pulse modulator has been operated to provide 100  $\mu$ s, 600 A arc pulses at over 200 Hz, although smaller values are used in the experimental results presented below.

Operated with the parameters given above, an erbia ( $\text{Er}_2\text{O}_3$ ) deposition rate of 1  $\mu\text{m/hr}$  has been achieved on a substrate of area 300  $\text{cm}^2$ , placed 28 cm from the cathode tip. This substrate intersected only a portion of the erbium plasma, so larger substrates could be coated. The arc pulse modulator can support substantially longer pulses at the arc current and frequency given above, so higher deposition rates can easily be achieved.

For ion implantation, the target is pulse biased with a high voltage modulator developed for our gaseous PSII research. The design of this modulator, which is based on the Litton 3408 hollow-beam switch tube, has been described elsewhere [11]. It can produce 20  $\mu$ s, 100 kV, 50 A pulses at 2 kHz, although when used to bias a cathodic-arc target we typically use 40 kV and pull maximum currents of 20 A. Operation of this target bias modulator can be synched to the operation of the cathodic-arc pulse modulator, with a time delay of up to 200  $\mu$ s, settable from the control panel.

### 3 Experimental Results

A simple measurement of bulk plasma velocity was performed by firing the cathodic-arc at an array of unbiased Langmuir probes, separated by distances varying between 5 cm and 20 cm. Electrons in the spatially and temporally

non-uniform plasma charge the probes negative, creating a jagged signal on an oscilloscope. This signal varies from shot to shot, but for any single shot is distinctive. Probes at differing positions pick up the same distinctive jagged signal, but with a temporal offset resulting from the time-of-flight between the probes. From this, a plasma velocity can be deduced. The bulk of the velocities thus derived fall in the range 1.2-2.5 cm/ $\mu$ s for carbon (corresponding to 9-40 eV), and 0.7-3.5 cm/ $\mu$ s for erbium (corresponding to 43-1100 eV). This species-independent velocity characteristic has been reported by a number of other groups [7, 12].

Particle-in-cell simulations performed with PDP1, a 1-d, bounded, electrostatic code [13], suggest that varying the delay between the target bias pulse and the cathodic-arc pulse should have a significant effect on the implanted ion current density and energy distribution. Figures 2 and 3 show the implanted ion current density and cumulative energy distribution, respectively, for a 20 cm long blob of  $10^{17}$  m<sup>-3</sup>, Er<sup>+2.5</sup> plasma with a drift of 1 cm/ $\mu$ s, that is, created by a 20  $\mu$ s arc pulse. These parameters were chosen to be similar to those existing in the laboratory experiment presented below. Two PIC simulations are shown, one in which the blob of plasma is in contact with the target, and one in which the leading edge of the blob of plasma is stood off 10 cm from the target, when the target is pulsed to 40 kV with a 4  $\mu$ s rise time. In both cases, a grounded surface is placed 40 cm from the target.

The plasma-in-contact case produces a typical PSII current density profile—a high initial peak which drops off as a space-charge-limited flow is established. A significant proportion of the ions in this case are implanted at energies lower than the expected 100 keV. In contrast, the plasma-stood-off case has a lower peak ion current density, and nearly all the ions are im-

planted near the full 100 keV energy. Some of the ions in the latter case are implanted at above 100 keV. This results from the plasma floating up in voltage with respect to the ground, although this effect is enhanced in this simulation by the electrons which are strongly heated by the non-physically sudden onset of the high voltage pulse. The reason for the differences in energy distribution can be seen in Figure 4, which shows the spatial potential profile present early in the target bias pulse. As soon as the target bias is applied, the electrons in the plasma move to shield the bulk of the plasma from electric fields. However, the applied potential must be dropped somewhere, and due to the limited spatial extent of the plasma, this occurs over the vacuum region and over the non-neutral region created by the motion of the electrons. In the plasma-in-contact case, the vacuum region is entirely behind the plasma, and most of the potential is dropped there early in the pulse. In addition, ions which are uncovered by the initial motion of the electrons are present throughout the sheath thus created, and do not all experience even the lower potential present across this sheath. Nevertheless, the ions do not have far to move to reach the target, resulting in the high initial current density in this case. This combination of high initial current density at relatively low energy accounts for the large proportion of low energy ions shown in Figure 3. In contrast, the potential is split between the vacuum regions in the plasma-stood-off case, so the ions are presented with a significant potential drop even early in the target bias pulse. This potential drop grows during the transit time of the ions across the stand-off region, so that ions have reached a relatively high energy by the time they are implanted into the target. Later in time, almost all of the potential is dropped across the plasma-target gap in both cases, as seen in Figure 5. In the plasma-in-contact case, this gap is the sheath which forms between

the plasma and target, but in the plasma-stood-off case, it is the residual stand-off distance.

The changes in ion current density seen in a laboratory experiment as the plasma stand-off is changed are similar to those from the PIC simulation. Each of Figures 6a-d show both the target bias voltage and target bias current waveforms for a series of implant pulses where the time delay between the cathodic-arc pulse and the target bias pulse has been increased by 20  $\mu$ s per figure. Each waveform shown in Figure 6a-d is the average over ten shots. In all cases, both the erbium cathodic-arc pulse and the target bias pulse last 20  $\mu$ s, and the arc current (not the plasma ion current) is 120 A. The target is a flat, circular aluminum plate of 8 inches diameter, placed 28 cm from the cathode. The cathode is surrounded by the grounded anode and vacuum chamber wall. The whole region between the cathodic-arc and the target is surrounded by a section of 8 inch diameter PVC pipe, to avoid depositing erbium all over the vacuum chamber. A component of the measured current in Figures 6a-d is due to secondary electrons released from the target, however, how much is not accurately known since the emission coefficient has not been directly measured. A comparison of implanted dose determined by integrating under the modulator current curves, with actual dose measured on silicon chips suggests that the emission coefficient may be as low as unity, although it could be higher if neutral erbium atoms were deposited as well. In the Figure 6a, the target bias pulse starts 5  $\mu$ s before the cathodic-arc pulse. The initial 4 A peak is due to charging of cables and a capacitor terminating the cable. The leading edge of the plasma requires 21  $\mu$ s to cross the cathode-target gap, and the 20  $\mu$ s plasma pulse has been drawn out to about 50  $\mu$ s by the time it reaches the target. This drawing out might be due to two effects. First, the range of plasma veloci-

ties quoted earlier in this paper would naturally result in a drawing out of the plasma blob with time. Second, the leading portions of the plasma are more influenced by the electric field present in the target-plasma gap during the target bias pulse, although this effect should be minimized because the sheath which forms on the leading edge of the plasma blob would shield the bulk of the plasma from this electric field. In Figure 6b, the target bias pulse has been delayed to 15  $\mu\text{s}$  after the cathodic-arc pulse, so that plasma does reach the target during its bias pulse. The transit time of the leading edge of the plasma is seen to be 20  $\mu\text{s}$ , about the same as the transit time in Figure 6a, suggesting that the sheath does, in fact, shield all but the ions at the very leading edge of the plasma. Given these effects, the transit times for the leading edge of the plasma are not inconsistent with the velocity measurements described earlier in this paper. In Figure 6c, the target bias pulse has been delayed to 35  $\mu\text{s}$  after the arc pulse. The plasma arrives earlier in the target bias pulse with increasing delay. The sudden drop in target bias current which is seen when the target bias voltage is shut off is believed to have its origins within the modulator, rather than being a plasma phenomena. However, the presence of a plasma does speed up the voltage drop of the target when the modulator is shut down. Our modulator does not utilize a "tail biter" to force the voltage down, relying instead on discharging through a set of resistors. The implantation of positive ions can discharge the modulator voltage faster than the characteristic RC discharge time through these resistors. Figure 6d, in which the target bias pulse has been delayed to 55  $\mu\text{s}$  after the arc pulse, corresponds most closely to the plasma-in-contact case shown in the PIC simulation. As in Figure 2, there is a high initial current peak resulting from the immediate implantation of ions very near the target. We hope to present, in a future paper, measurements

of ion energy distribution at the target which correspond to the differences shown in the PIC simulations shown in Figure 3.

## 4 Summary and Conclusions

A cathodic-arc has been combined with an existing PSII experiment to allow high energy implantation of erbium ions. The target bias modulator is synchronized with the cathodic-arc pulse modulator with a variable time delay between the two. This variable delay allows the plasma drift time between the cathode and target to be exploited to change the load on the target bias modulator, an effect which is seen in both PIC simulations and laboratory experiment. PIC simulations also suggest that this delay can be used to change the energy distribution of the implanted ions.

## 5 Acknowledgments

We are indebted to David Miera who constructed our cathodic-arc pulse modulator, and to Joe Garcia and Ralph Romero who machined and assembled the fixturing for our experiment. Don Rej contributed a number of useful observations about this research. This work is supported by the U.S. Department of Energy.

## References

- [1] J. R. Conrad, *J. Appl. Phys.* 62 (1987) 777.
- [2] J. R. Conrad, J. L. Radtke, R. A. Dodd, Frank J. Worzala, and Ngoc C. Tran, *J. Appl. Phys.* 62 (1987) 4591.
- [3] G. A. Collins, R. Hutchings, and J. Tendys, *Mat. Sci. Engr.* A139 (1991) 171.
- [4] D. J. Rej, J. R. Conrad, R. J. Faehl, R. J. Gribble, I. Henins, N. Horswill, P. Kodali, M. Nastasi, W. A. Reass, M. Shamim, K. Sridharan, J. R. Tesmer, K. C. Walter, and B. P. Wood, *Proc. MRS Symp.* 316 (1994) 593.
- [5] A. Anders, S. Anders, I. G. Brown, M. R. Dickinson, and R. A. MacGill, *J. Vac. Sci. Technol.* B12 (1994) 815.
- [6] I. G. Brown, A. Anders, S. Anders, M. R. Dickinson, and R. A. MacGill, *J. Vac. Sci. Technol.* B12 (1994) 823.
- [7] A. S. Gilmour, Jr. and D. L. Lockwood, *Proc. IEEE* 60 (1972) 977.
- [8] I. G. Brown, *Rev. Sci. Instrum.* 65 (1994) 3061.
- [9] B. P. Wood, I. Henins, R. J. Gribble, W. A. Reass, R. J. Faehl, M. A. Nastasi, and D. J. Rej, *J. Vac. Sci. Technol.* B12 (1994) 870.
- [10] B. P. Wood, J. T. Scheuer, M. A. Nastasi, R. H. Olsher, W. A. Reass, I. Henins, and D. J. Rej, *Proc. MRS Symp.* 279 (1993) 345.
- [11] W. A. Reass, *J. Vac. Sci. Technol.* B12 (1994) 854.

- [12] A. A. Plyutto, V. N. Ryzhkov, and A. T. Kapin, *Sov. Phys. JETP* 20 (1965) 328.
- [13] C. K. Birdsall, *IEEE Trans. Plasma Sci.* 19 (1991) 65.

## Figure Captions

Figure 1. Schematic diagram of the cathodic-arc.

Figure 2. Ion current density in a 1-D PIC simulation of a target pulsed to -40 kV with a 4  $\mu\text{s}$  rise time in a  $10^{17} \text{ m}^{-3}$ ,  $\text{Er}^{+2.5}$  plasma with a drift toward the target of 1  $\text{cm}/\mu\text{s}$ . The plasma is 20 cm in length in a target-ground gap of 40 cm. For the dotted curve, the plasma is in contact with the target when the bias pulse is applied. For the solid curve, the plasma is 10 cm away from the target when the bias pulse is applied.

Figure 3. Cumulative implanted ion energy distribution under the same simulation conditions as in Figure 2.

Figure 4. Spatial potential profile after 0.5  $\mu\text{s}$ , for the same simulation conditions as in Figure 2.

Figure 5. Spatial potential profile after 5  $\mu\text{s}$ , for the same simulation conditions as in Figure 2.

Figures 6a-d. Experimental target bias voltage and current for a 20  $\mu\text{s}$  erbium cathodic-arc pulse directed at a 300  $\text{cm}^2$  flat aluminum target placed 28 cm from the cathode. With respect to the cathodic-arc pulse, the target bias pulse was a) advanced 5  $\mu\text{s}$ , b) delayed 15  $\mu\text{s}$ , c) delayed 35  $\mu\text{s}$ , and d) delayed 55  $\mu\text{s}$ .

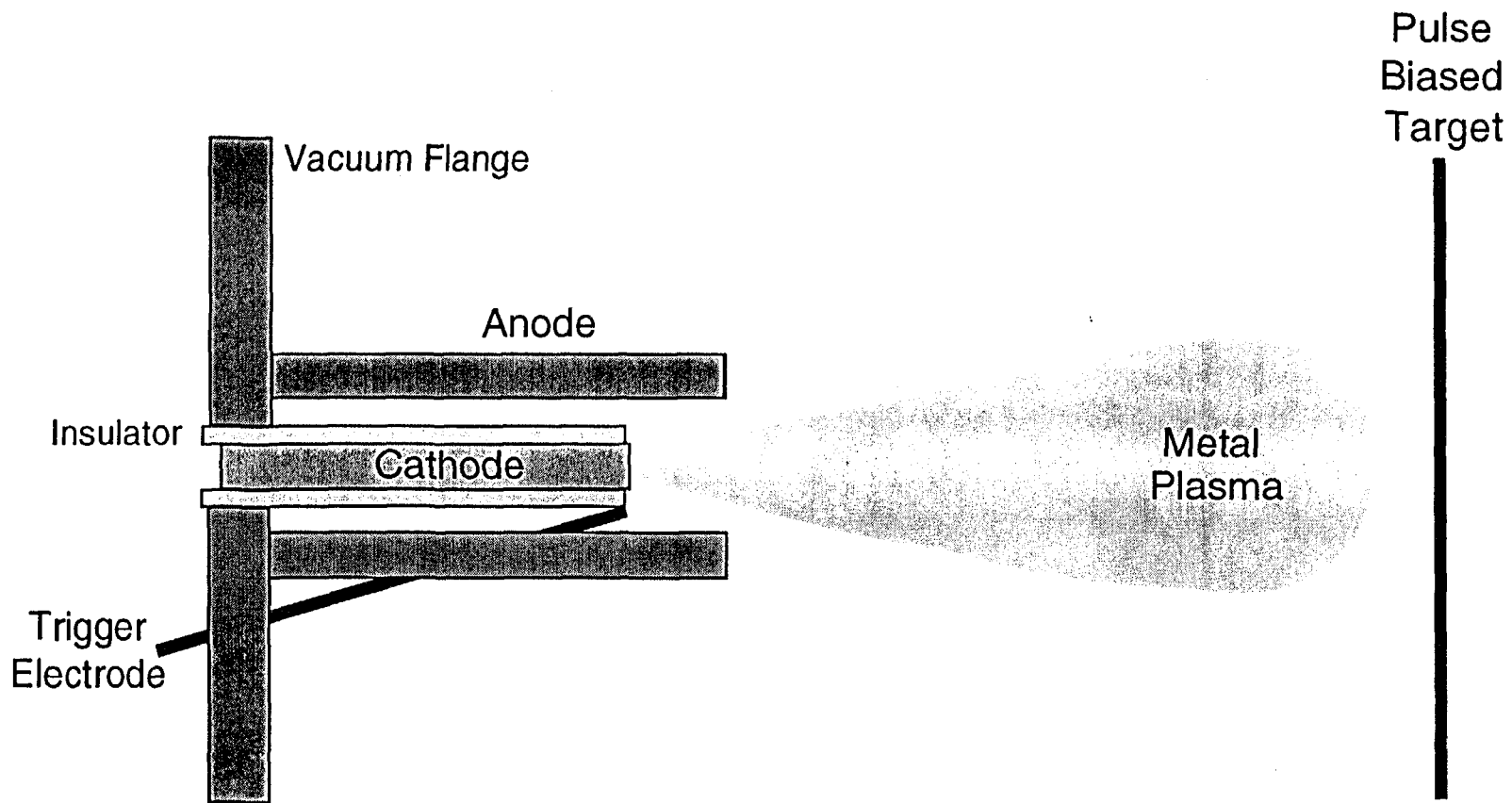


Figure 1

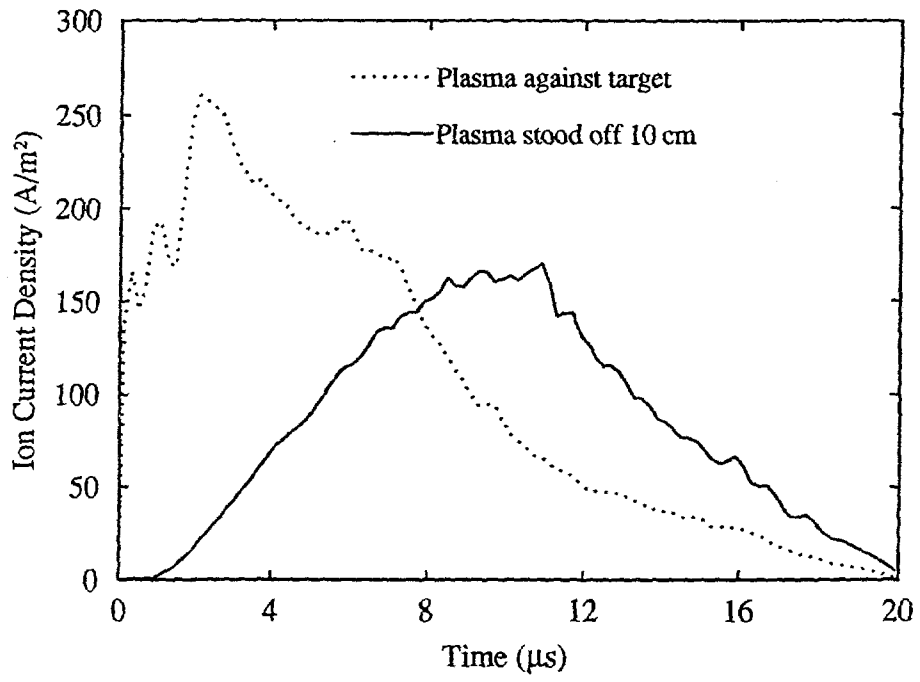


Figure 2

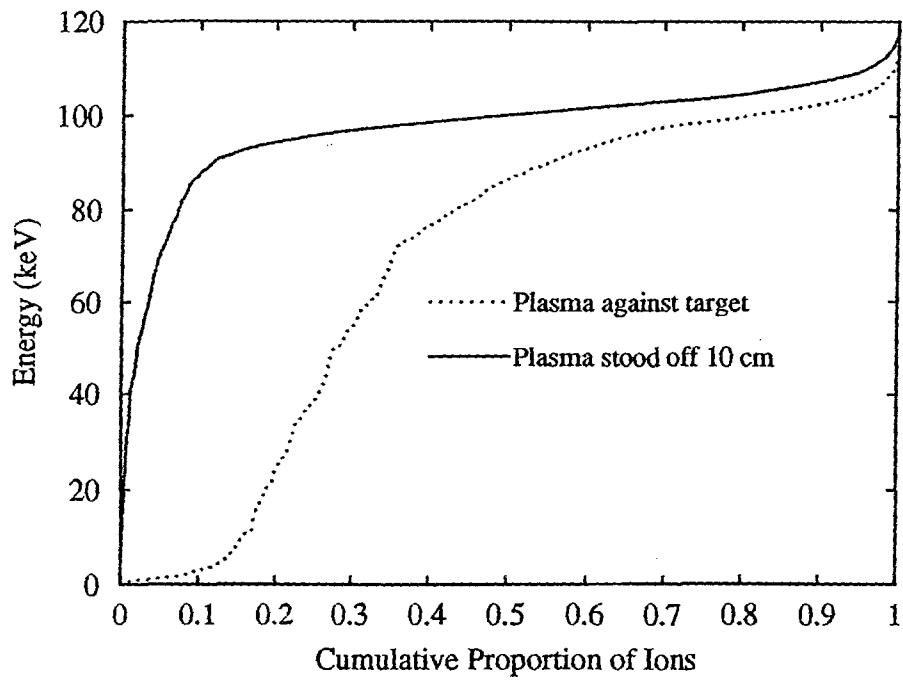


Figure 2

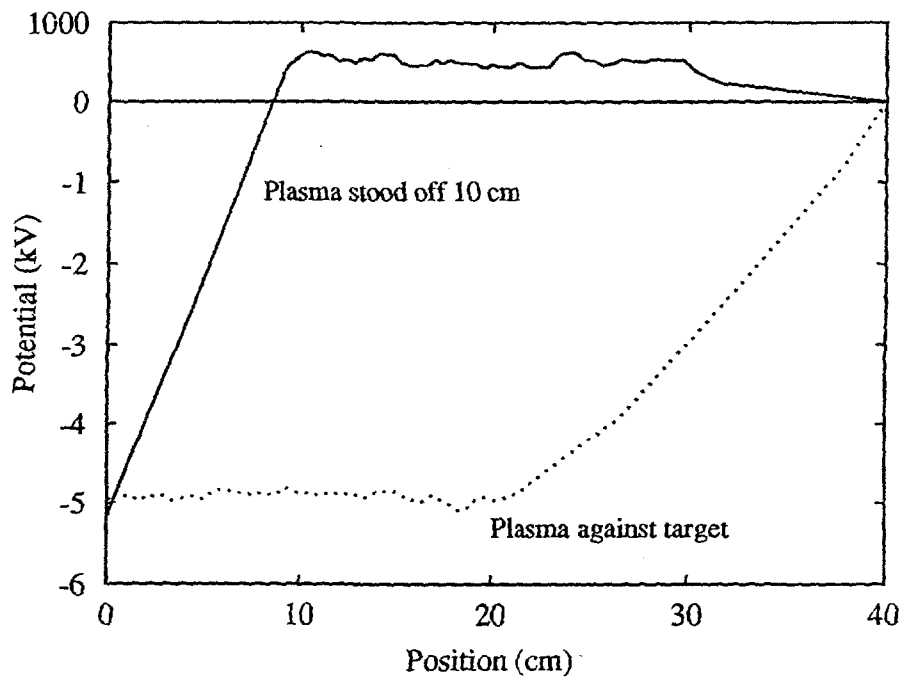
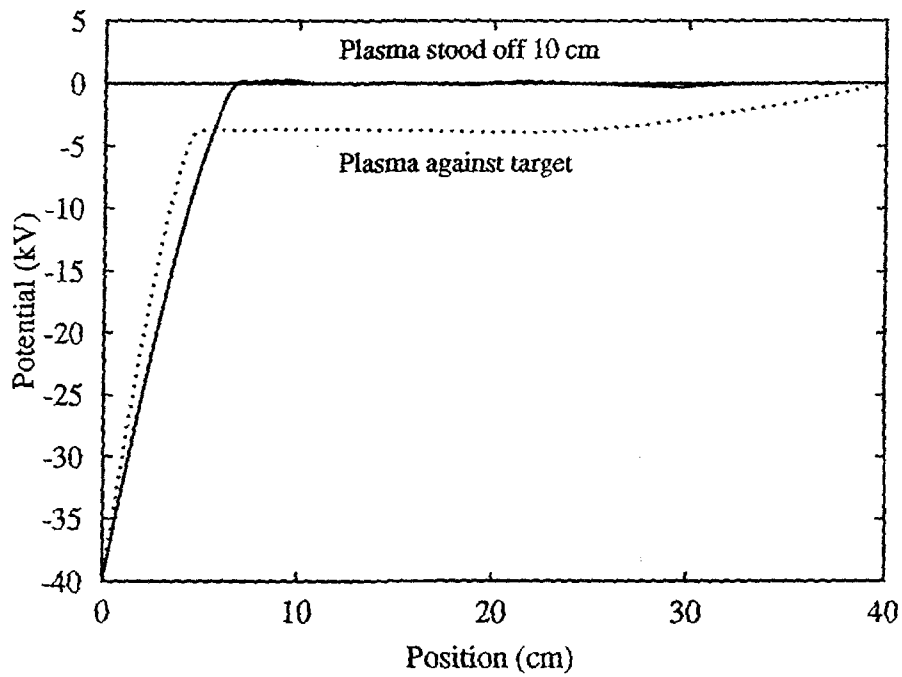


Figure 11



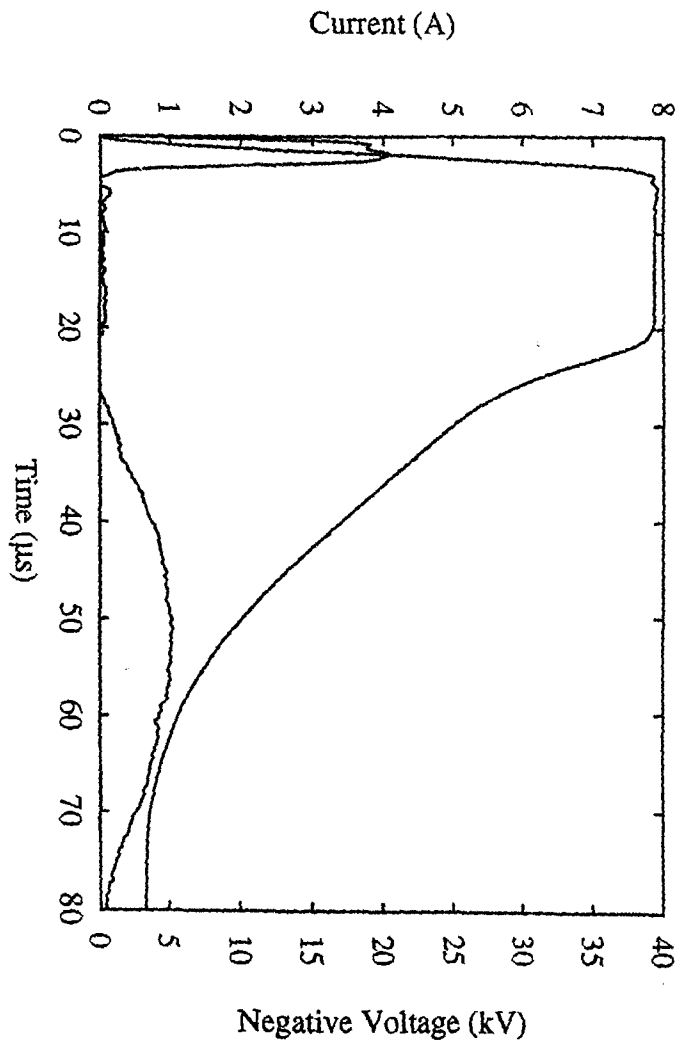
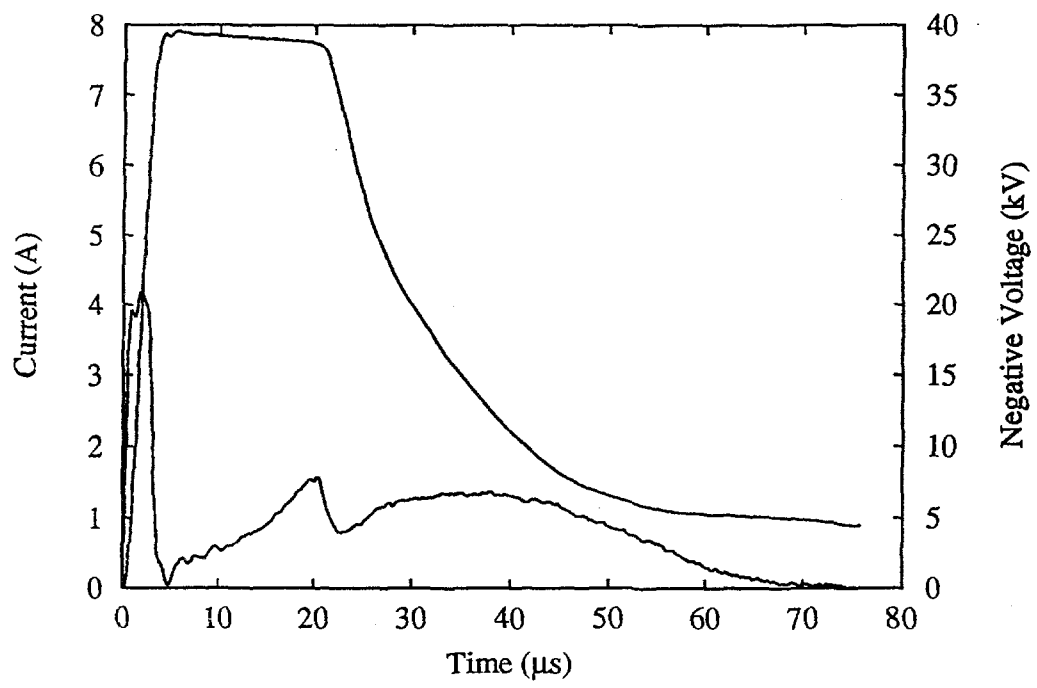


Figure 1



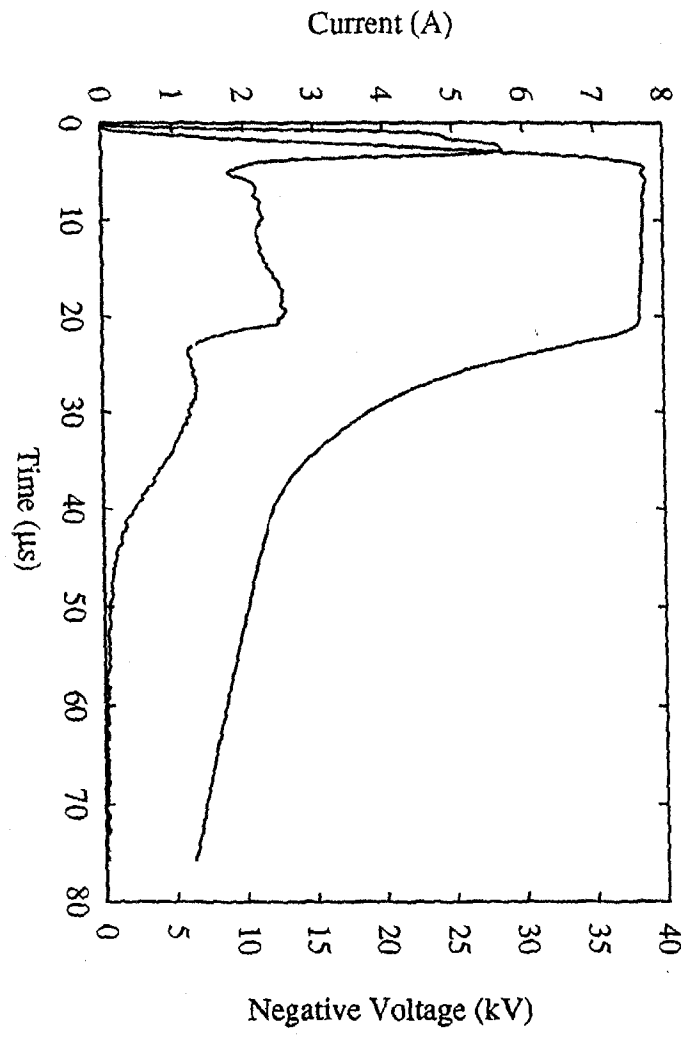


Figure 1

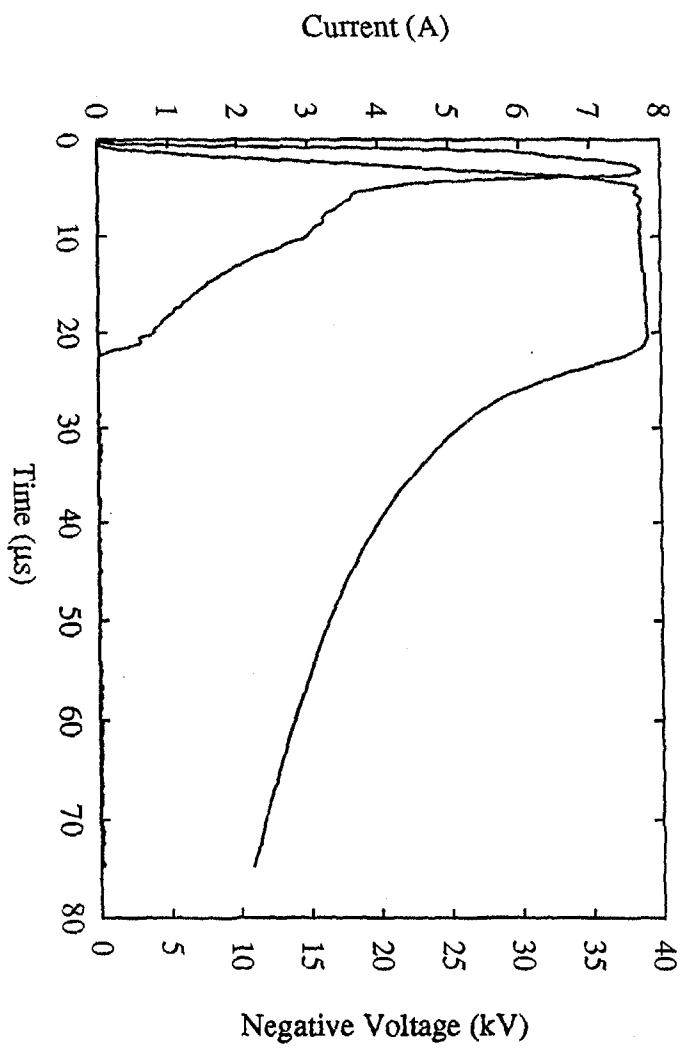


Figure 6d